Solar Energy Materials & Solar Cells 94 (2010) 484–491

Contents lists available at ScienceDirect

Solar Energy Materials & Solar Cells

journal homepage: www.elsevier.com/locate/solmat

Effect of shifting of aromatic rings on charge carrier mobility and photovoltaic response of anthracene and thiophene-containing MEH-PPE-PPVs

Serap Günes [a,*], Andreas Wild [b,c,d], Emel Cevik [a], Almantas Pivrikas [e], Ulrich S. Schubert [b,c,d], Daniel A.M. Egbe [e]

[a] Yildiz Technical University, Faculty of Arts and Science, Department of Physics, Davutpasa Campus, 34210, Esenler, Istanbul, Turkey
[b] Laboratory of Organic and Macromolecular Chemistry, Friedrich-Schiller-University Jena, Humboldtstr.10, D-07743 Jena, Germany
[c] Laboratory of Macromolecular Chemistry and Nanoscience, Eindhoven University of Technology, PO Box 513, 5600 MB Eindhoven, The Netherlands
[d] Dutch Polymer Institute (DPI), PO Box 902, 5600 AX Eindhoven, The Netherlands
[e] Linz Institute for Organic Solar Cells (LIOS), Johannes Kepler University Linz, Physical Chemistry, Altenberger Strasse 69, A-4040, Linz, Austria

ARTICLE INFO

Article history:
Received 13 October 2009
Received in revised form
11 November 2009
Accepted 12 November 2009
Available online 8 December 2009

Keywords:
Polymer solar cells
Conjugated polymers
Organic solar cells

ABSTRACT

We have investigated the charge carrier mobility and photovoltaic response of two thiophene-[**P1** (MEH-PPE_1-$PThV_2$) and **P2** (MEH-$PThE_1$-PPV_2)] as well as two anthracene-containing poly (phenylene-ethynylene) family of polymers [**P3** (MEH-PPE_1-$PAnV_2$) and **P4** (MEH-$PAnE_1$-PPV_2)], whereby the position of thiophene or anthracene has been shifted from between two double bonds (**P1** and **P3**) to the bridge between triple bond and double bond (**P2** and **P4**). **P2** shows better photovoltaic performance than **P1**, whereas similar photovoltaic characteristics were found for **P3** and **P4**. The devices using the blends of **P2** as donor and PCBM as acceptor (1:3 weight ratio) exhibited a short-circuit current density of J_{SC}=5.2 mA/cm^2, an open-circuit voltage of V_{OC}=800 mV, fill factor FF=0.44 and resulting power conversion efficiency $\eta_{AM\ 1.5}$=1.8%.

1. Introduction

Organic solar cell research has attracted worldwide attention during the last two decades. Organic semiconductors are easily processable, light weight, easy to integrate in a wide variety of devices and have chemically tunable properties.[1] These properties describe the advantages of organic "plastic" solar cells over that of conventional silicon solar cells.

Conjugated polymers, also known as semiconducting polymers, are distinguished by alternating single and double bonds between carbon atoms on the polymer backbone [2]. Polymeric organic solar cells mainly consist of an electron-donating conjugated polymeric material and an electron-accepting material, to make a mutually percolating structure with interpenetrating networks [3,4,5].

Among π-conjugated polymers, polythiophenes are promising candidates not only for organic solar cells but also for other optoelectronic devices such as light emitting diodes and field effect transistors (OFETs).[6] At present, the commonly used polythiophene derivatives, as the electron donor in polymer solar cells, are mainly poly(3-hexylthiophene) (P3HT) and poly (3-octylthiophene) (P3OT) [7,8,9]. Recently, Heeger et al. demonstrated 6.1% bulk heterojunction solar cells with internal quantum efficiency reaching 100% [10]. Research on the subject of organic solar cells has focused on improving the power conversion efficiency of laboratory type organic solar cells and also focuses on the operational stability that can be achieved under ideal conditions [11–15]. The improvement in organic solar cells creates a demand for advanced materials with better absorption and transport properties. The main efforts for improvement are based on designing and developing new generation of materials among conjugated polymers [16].

In this study, we have investigated the hole mobility and the photovoltaic performance of two thiophene-containing polymers [poly{(1,4-(5-(2-ethylhexyl)oxy)-2-methoxy)-phenylene-ethynylene-1,4-(5-[(2-ethylhexyl)oxy]-2-methoxy)phenylene-vinylene-2,5-thiophenylene-vinylene} (MEH-PPE_1-$PThV_2$) (**P1**) and poly(1,4-(5-(2-ethylhexyl)oxy)-2-methoxy)-phenylene-ethynylene-2,;5-thiophenylene-vinylene-1,4-(5-(2-ethylhexyl);oxy)-2-methoxy);-phenylene-vinylene) (MEH-$PThE_1$-PPV_2) (**P2**)] as well as two anthracene-containing polymers [poly{1,4-(5-[(2-ethylhexyl)oxy]-2-methoxy) phenylene-ethynylene-1,4-(5-[(2-ethylhexyl)oxy]-2-methoxy)phenylene-vinylene-9,10-anthracenylene-vinylene}(MEH-PPE_1-$PAnV_2$) (**P3**) and poly {(1,4-(5-(2-ethylhexyl)oxy)-2-methoxy)-phenylene-ethynylene-9,10-anthracenylene-vinylene-1,4-[(5-(2-ethylhexyl) oxy)-2-methyloxy]-phenylene-vinylene} (MEH-$PAnE_1$-PPV_2) (**P4**)]. The difference between **P1** and **P2** as well as between **P3** and **P4** lies in the position of thiophene or anthracene in polymeric backbone.

* Corresponding Author. Tel.: +90 212 383 4236; fax: +90 212 449 1514.
E-mail address: sgunes@yildiz.edu.tr (S. Günes).

0927-0248/$ - see front matter © 2009 Elsevier B.V. All rights reserved.
doi:10.1016/j.solmat.2009.11.011

In this work, we have evaluated the photovoltaic performance of the **P1–P4** as donor materials with respect to (1) the position of either thiophene or anthracene within the conjugated backbone and (2) the density of the hydrophobic side chains around the conjugated backbone. The devices using the blends of **P2** and PCBM with 1:3 ratio showed J_{SC} of 5.2 mA/cm^2, a V_{OC} of 800 mV and fill factor of 0.44 which corresponds to the power conversion efficiency of 1.8%.

2. Experimental

The synthesis, molar masses thin film optical and electrochemical characteristics of the four polymers have been described elsewhere [17]. The chemical structures are depicted in Fig. 1 while Table 1 summarizes the SEC, optical and electrochemical data.

For solar cell preparation, as substrates, glass sheets of 1.5 cm × 1.5 cm covered with ITO, from Merck KG Darmstadt, were used with an ITO (indium tin oxide) and sheet resistance $< 15\ \Omega\text{cm}^{-2}$. The ITO was patterned by etching with an acid mixture of HCl:HNO_3:H_2O (4.6: 0.4: 5) for 30 min. The part of the substrate which forms the contact is covered with a scotch tape to prevent etching. The tape was removed after etching and the substrate was then cleaned using acetone and *iso*propanol in an ultrasonic bath.

Poly(3,4-ethylenedioxythiophene)–poly(styrenesulfonate) (PEDOT:PSS) was spin coated on the glass–ITO substrate, and dried under a dynamic vacuum.

The blends for the active layer with 1:1, 1:2, 1:3 or 1:4 (w:w) ratios of **PX**/PCBM (**X** stands for **1**, **2**, **3** and **4**), prepared by dissolving 6 mg of polymer and 12 mg of PCBM (in the case of 1:2) in 1 ml of chlorobenzene (CB) and stirring at 50 °C overnight. For the top electrodes, 0.6 nm of lithium fluoride (LiF) and 100 nm of Aluminum (Al) were thermally evaporated.

All current–voltage (*I–V*) characteristics of the PV devices were measured using a Keithley SMU 236 under nitrogen in a dry glove box. A Steuernagel solar simulator for AM1.5 conditions was used as the excitation source with an input power of 100 mW/cm^2 white-light illumination which was calibrated using a standard crystalline silicon diode. The solar cells were illuminated through the ITO side.

The evaluation of the solar cells was carried out by using the power conversion efficiency.

$$\eta_{AM1.5}(\%) = \left(\frac{P_{out}}{P_{in}}\right) \times 100 = \frac{FFxV_{oc} \times J_{sc}}{P_{in}} \times 100.$$

The percentage efficiency, $\eta_{AM1.5}$, is given by the ratio of the power output (P_{out}), to the power input from the solar simulator (P_{in}, 100 mW/cm^2). The output power of a solar cell under illumination is the product of the fill factor FF, the open-circuit voltage V_{OC} (V) and the current density under short-circuit conditions J_{SC} (mA/cm^2). The fill factor is obtained using the following equation:

$$FF = \frac{V_{mpp} \times J_{mpp}}{V_{oc} \times J_{sc}},$$

where maximum power point of the product of the voltage and the current density (V_{mpp} and J_{mpp}) is divided by the product of the open-circuit voltage and the short-circuit current.

The spectrally resolved photocurrent was measured with an EG&G Instruments 7260 lock-in amplifier. The samples were illuminated with monochromatic light of a Xenon lamp. The incident photon to current efficiency (% IPCE) was calculated according to the following equation:

$$\text{IPCE}(\%) = \frac{I_{sc} \times 1240}{P_{in} \times \lambda_{incident}},$$

Table 1
SEC thin film optical and electrochemical data of **P1–P4**.[17].

Code	M_n[g/mol]	M_w/M_n	P_n	λ_a[nm]	$E_g^{opt\ b)}$[eV]	HOMO [eV]	LUMO [eV]	E_g^{elc} [eV]
P1	16 600	1.9	26	508	2.11	5.17	3.23	1.94
P2	32 500	2.3	52	499	2.11	5.15	3.15	2.00
P3	33 000	2.4	46	453	2.22	5.21	3.23	1.98
P4	31 000	2.5	43	506	2.05	5.23	3.35	1.88

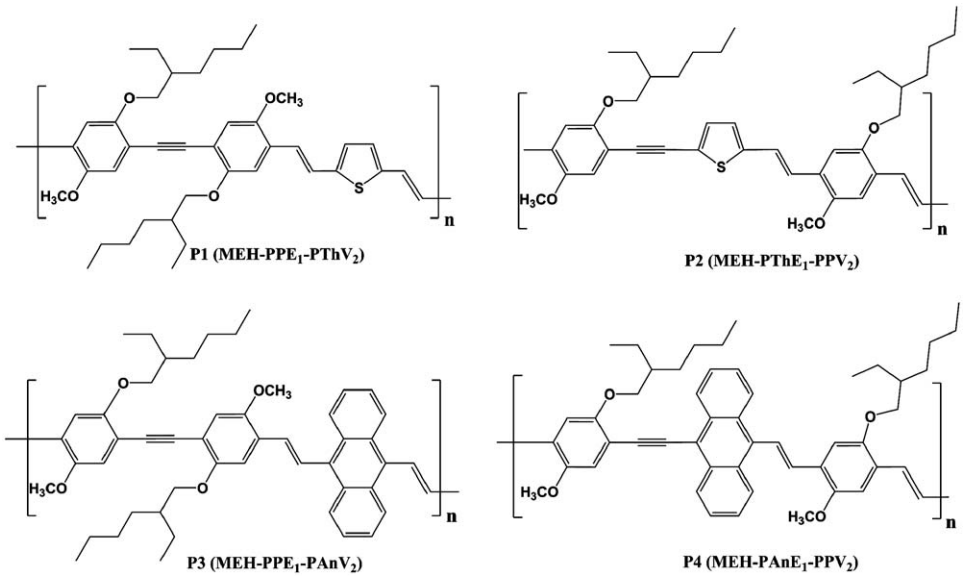

Fig. 1. Chemical structures of the polymers.

where I_{SC} ($\mu A/cm^2$) is the measured current under short-circuit conditions of the solar cell, P_{in} (W/m^2) is the incident light power, measured with a calibrated silicon diode, and λ (nm) is the incident photon wavelength.

Atomic force microscopy studies were performed using Digital Instruments DIMENSION 3100 in the tapping mode.

Sandwich-type samples were prepared for charge carrier mobility measurements. The solutions were filtered through a 0.45 μm filter before deposition by spin coating or drop casting on top of pre-patterned ITO-covered glass substrates. Subsequently, 100 nm aluminum top contacts were evaporated on top of the polymer (vacuum 10^{-6} mbar). Samples were prepared under inert atmosphere and the films were measured *in vacuum* using an optical cryostat (Oxford Optistat DNV). Thicknesses for thin films (spin coated) were on the order of several hundred of nanometers whereas for thick films (drop cast) on the order of several micrometers. For the CELIV experiments a variable pulse generator (Agilent 33250A) and oscilloscope (Tektronix TDS 754C) were used to record the current transients. For triggering purposes to ensure the proper delay time between voltage and light pulse, a pulse and the delay function generator (Stanford DG535) was used. A Nd:YAG laser (Coherent Infinity 40 – 100) was employed to photogenerate the charge carriers using a 5 ns laser pulse at a wavelength of 355 nm.

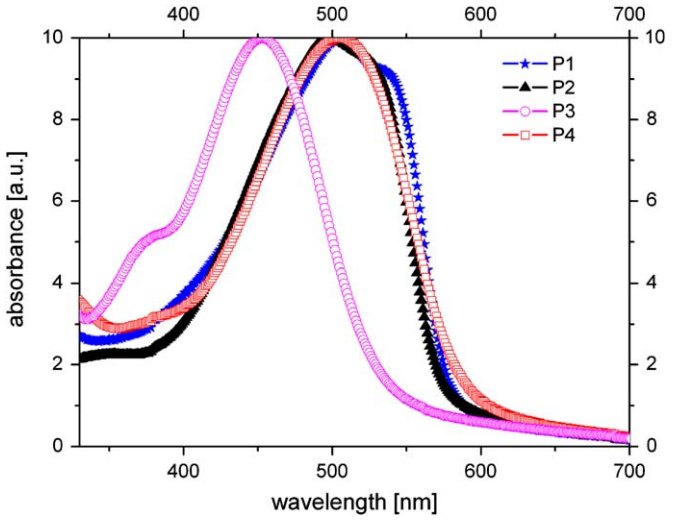

Fig. 2. Optical absorption spectra of thin films of pristine polymers **P1–P4**.

3. Results and discussion

Optical absorption spectra of the pristine polymers **P1**, **P2**, **P3** or **P4** are shown in Fig. 2.

Transparent thin films of the polymers were spin-casted on a quartz glass substrate from a chlorobenzene solution (concentration 10^{-3}–10^{-2} M), leading to thicknesses between 100 and 150 nm. The difference between **P1** and **P2** as well as between **P3** and **P4** lies in the position of thiophene or anthracene in polymeric backbone. Despite the difference in the chemical structure, polymers **P1** and **P2** exhibit nearly identical absorption spectra both in solution and thin film [17]. The absorption spectra of the anthracene-containing polymers **P3** and **P4** differ clearly. When the position of anthracene is shifted from between two double bonds (**P3**) to the bridge between double bond and triple bond (**P4**) a bathochromic shift of 53 nm occurs, which is

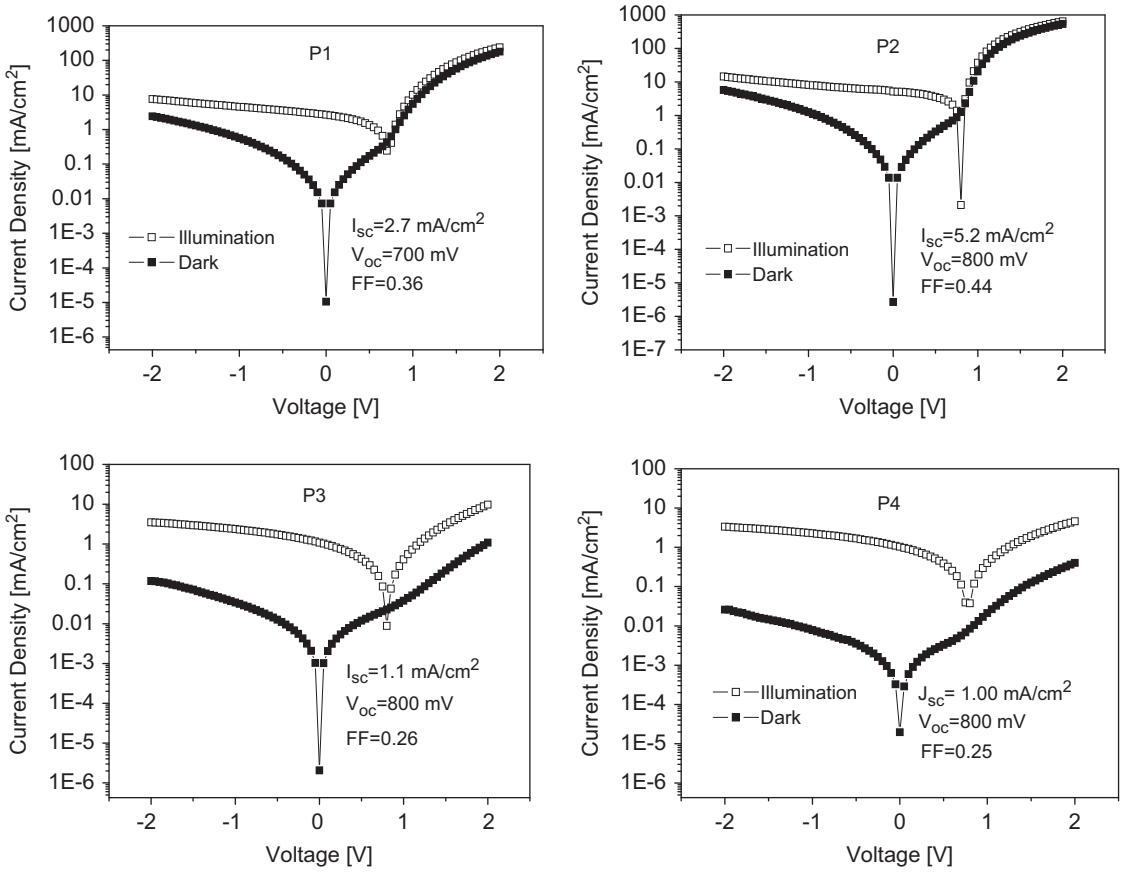

Fig. 3. Current–voltage characteristics of **P1**:PCBM, **P2**:PCBM, **P3**:PCBM and **P4**:PCBM with 1:3 wt ratio.

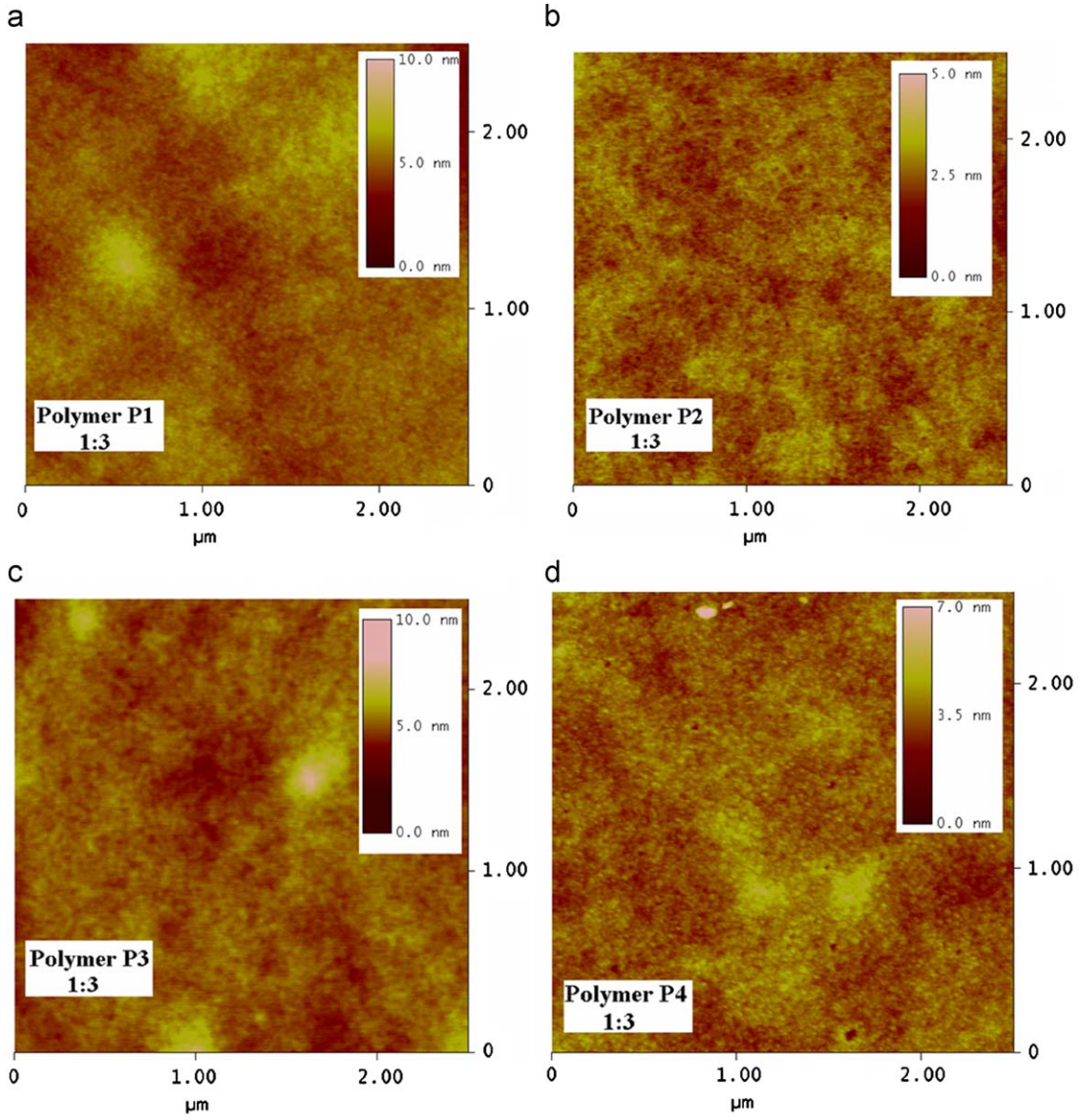

Fig. 4. AFM images of blend films of different polymers with PCBM spin cast from chlorobenzene (a) polymer **P1**:PCBM, (b) polymer **P2**:PCBM, (c) polymer **P3**:PCBM and (d) polymer **P4**:PCBM with 1:3 wt ratio.

attributed to the extension of conjugation in the same order. This results from a significant steric interaction between the hydrogen atoms in the 1, 4, 5 and 8 positions and the vinylenic protons that causes a torsion about the (formal) single bonds and thus decreases the conjugation along the main chain [18].

This positional difference has led to ca 50 nm bathochromic shift of the absorption maximum, when comparing the anthracene-containing materials **P3** with **P4**, due to different level of distortion around the anthracene unit in both compounds. This was not the case for the thiophene-containing compounds **P1** and **P2**, where virtually no difference in their optical absorption behavior was observed, presumably as a result of the strong tendency of thiophene to induce planarization [17].

P1–P4 have been investigated as possible donors in organic solar cells. The current–voltage (I–V) characteristic curves in dark and under illumination (under AM1.5 conditions) of ITO/PEDOT:PSS/Polymer:PCBM/LiF/Al (1:3 wt ratios) are shown in Fig. 3.

Among these four polymers **P2** showed far better performance with a power conversion efficiency of 1.8% than those from **P1**, **P3**

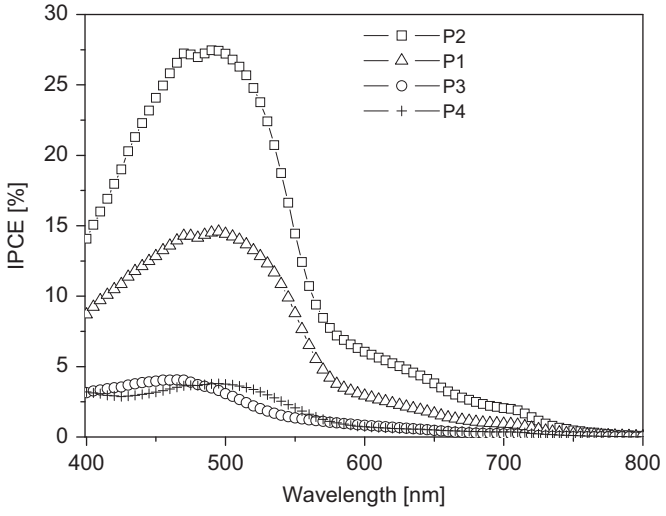

Fig. 5. IPCE spectra of the solar cells (**P1**:PCBM, **P2**:PCBM, **P3**:PCBM, **P4**:PCBM blends with 1:3 ratio).

and **P4**. They exhibit open-circuit voltages (V_{OC}), as high as 800 mV. Although there are still discussions on the nature of V_{OC} in literature, V_{OC} is known to be proportional to the difference between the HOMO of the donor and the LUMO of the acceptor. HOMO and LUMO levels of the investigated polymers are shown in Table 1. Considering the LUMO level of PCBM as 4.2 eV, [19] theoretical values of V_{OC} are calculated as 0.97, 0.95, 1.01 and 1.03 for **P1**, **P2**, **P3** and **P4**, respectively. In this study, the V_{OC} of the devices was found to be around 0.8 V for **P2**, **P3** and **P4** and 0.7 V for **P1**.

The behavior of solar cells can be better analyzed via understanding the nanomorphology of the active layer. The challenge in bulk heterojunction solar cells is to organize donor and acceptor materials in a nanometer scale. On one hand, their interfacial area shall be maximized, while typical dimensions of phase separation shall stay within the exciton diffusion length (in the order of 10 nm) [20]. On the other hand, continuous, preferably undisturbed pathways for transport of charge carriers to the electrodes must be ensured [21].

To correlate the morphology of the solar cells to the photovoltaic performance, we performed an AFM study on polymer:PCBM blends. Fig. 4 shows the height images obtained by AFM for polymer:PCBM films 1:3 wt ratios spin cast from chlorobenzene.

The films consisting of P1, P2, P3 and P4 with 1:3 blend ratios have roughness (height scale) values varying between 5 and 10 nm which indicate smooth surfaces. The films of P4:PCBM blends seem to lack hole-like structures which might be the reason for the lowest performance of all. For all blend films no apparent phase separation was observed. However, among four polymer:PCBM films, **P2**:PCBM films indicate the smoothest surface which was derived from the height scale values (5 nm for **P2**). Such a fine blending of the donor and acceptor components in a bulk heterojunction can result in increased carrier recombination, which would explain the low filling factor (below 0.5) of the four polymers. Similar results were also observed in a study by Kopidakis et al. [22]. On the other hand P4:PCBM blend films contain hole-like structures on the surface which might be an indication for film formation problems on PEDOT:PSS covered ITO surface and this might lack the device performance.

IPCE shows how many percent of photons at a given wavelength create charges that reach the electrodes. Fig. 5 shows the IPCE for **P1**:PCBM, **P2**:PCBM, **P3**:PCBM and **P4**:PCBM with 1:3 ratio.

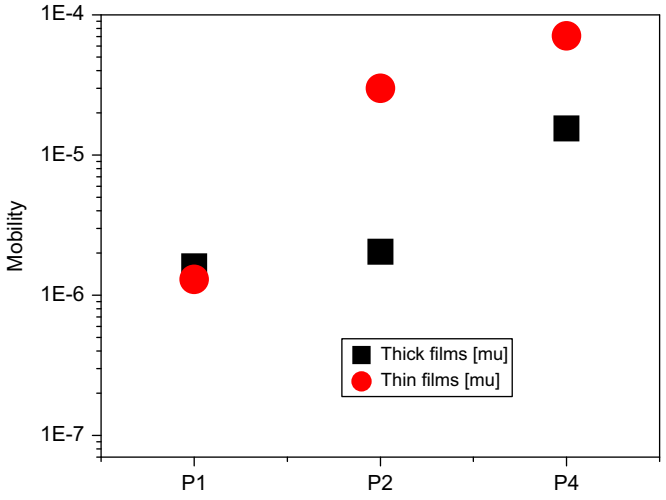

Fig. 6. Hole mobility vs investigated polymers.

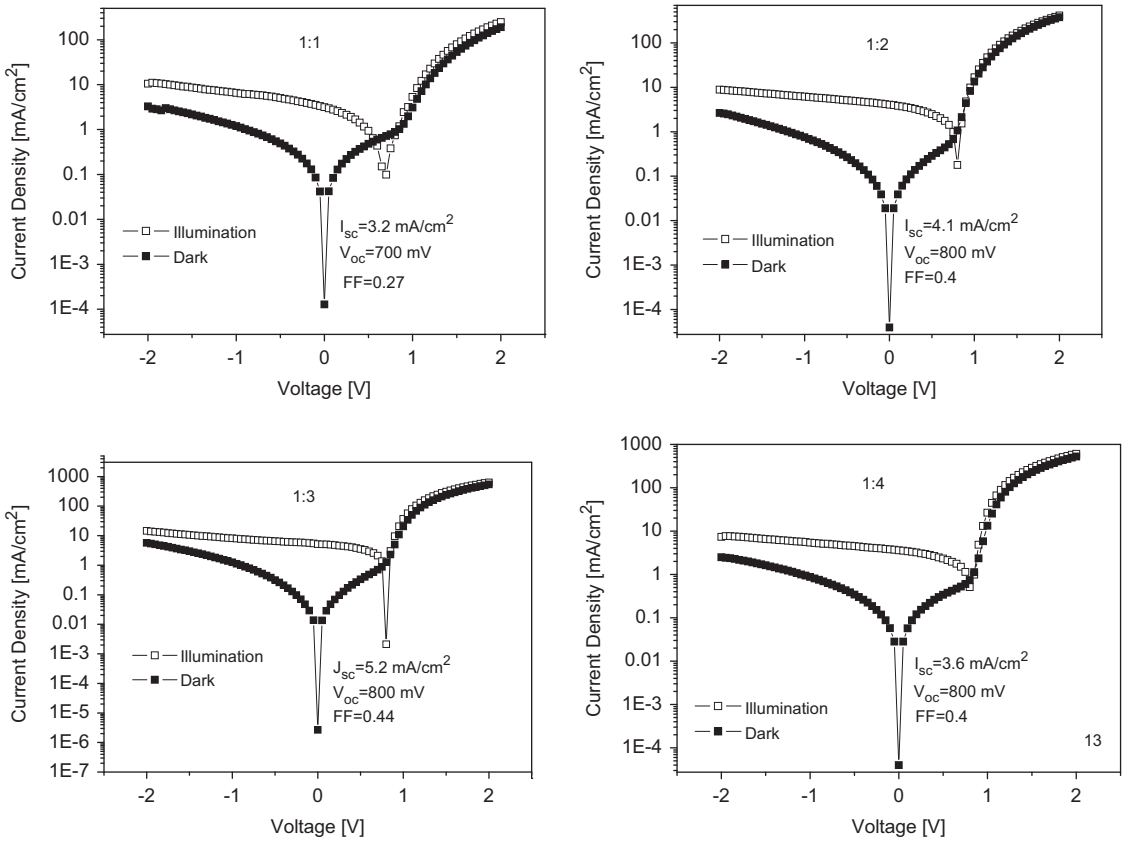

Fig. 7. Current–voltage characteristics of **P2:**PCBM 1:1, 1:2, 1:3 and 1:4 ratios.

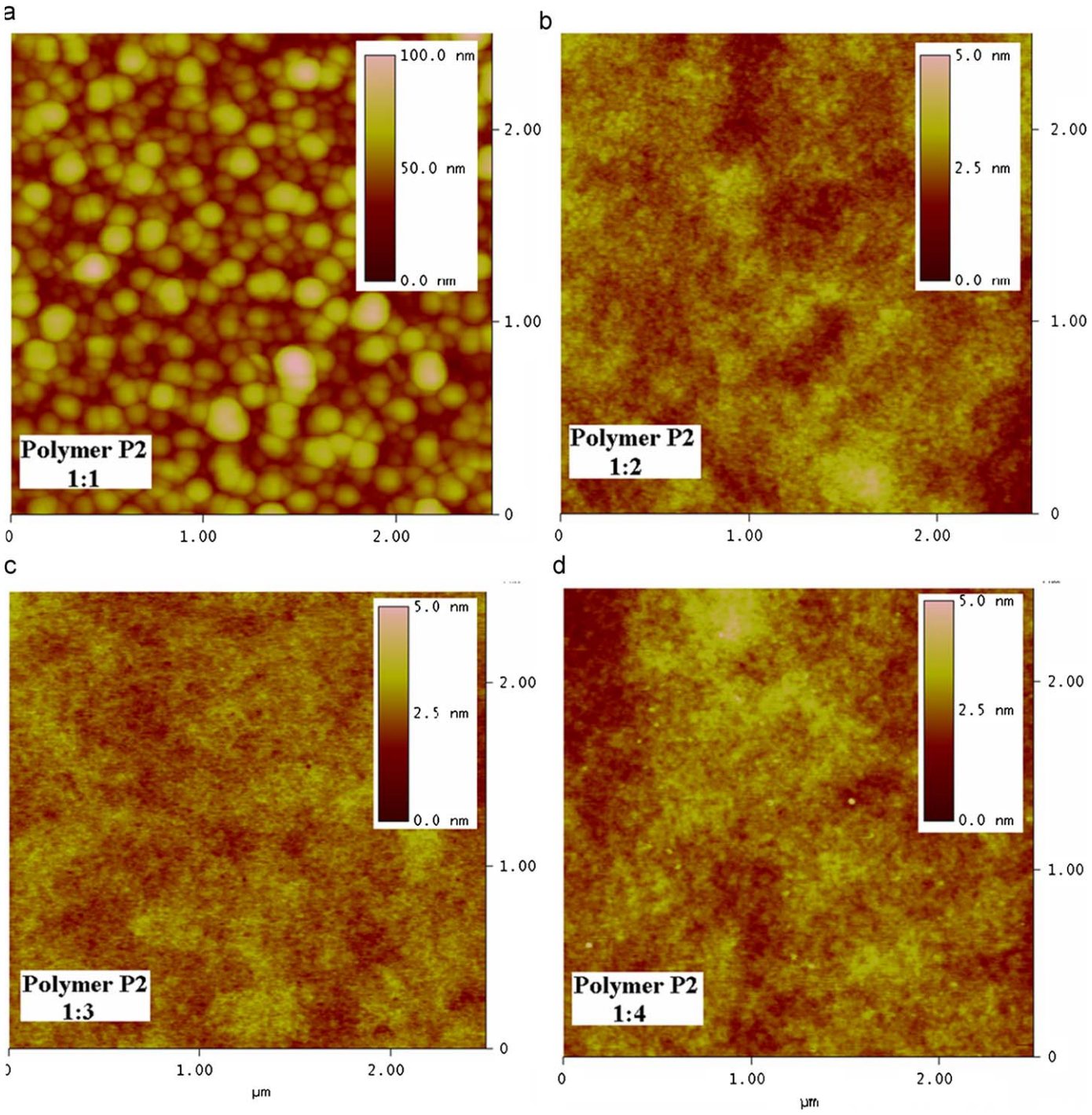

Fig. 8. AFM images of polymer **P2**:PCBM blend films for different wt ratios (a) 1:1, (b) 1:2, (c) 1:3, (d) 1:4.

The % IPCE plot exhibits a maximum photocurrent contribution of ca. 30%, 14%, 5% and 4% at around 500 nm for **P2**, **P1**, **P3** and **P4**, respectively, which is in accordance with the photovoltaic performance. It is noted that the spectrum lies over a wide range of wavelengths, 350–750 nm in agreement with the absorption spectra in Fig. 2 above.

To correlate the photovoltaic performance to the mobility of the polymers we performed mobility measurements on pristine polymers. The hole mobility graph and values of the investigated polymers are shown in Fig. 6 and Table 2, respectively. When trying to relate the mobility of carriers to the photovoltaic performance, it is very important to know the slower charge carrier mobility which dominates the total transport in the device. It has been also shown that the dispersive charge transport in pristine polymers becomes non-dispersive when PCBM is added to the blend [23].

However, relating mobility in pristine films and in bulk-heterojunctions might be very difficult due to strong morphology dependence of carrier mobility. On the other hand, the trend of mobilities should be similar in pristine polymer films and in organic solar cells. Among the investigated polymers **P4** and **P2** had the highest carrier mobility even though **P4** shows the worst photovoltaic performance. The composition dependence between the polymer and PCBM strongly influences the charge transport

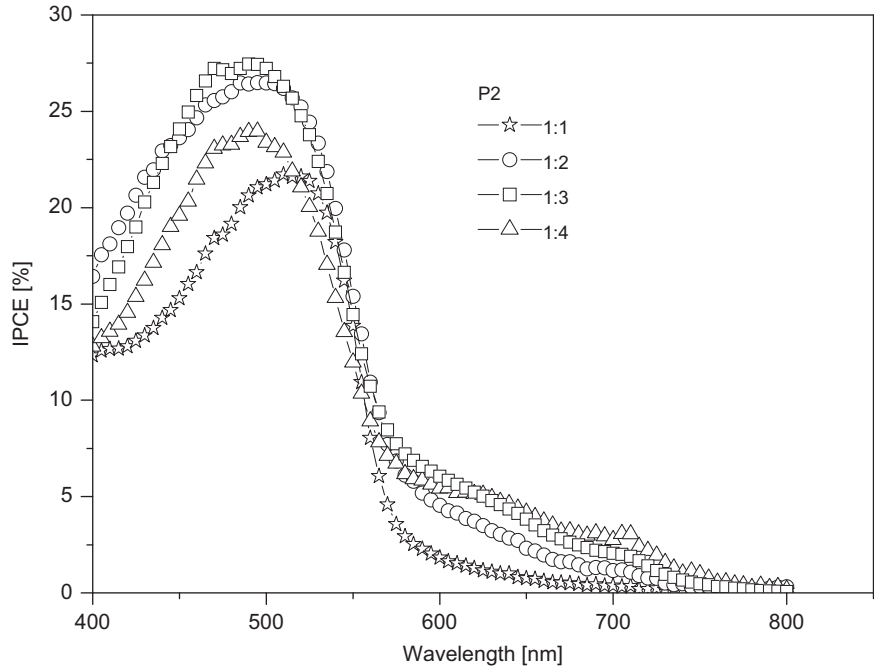

Fig. 9. IPCE for **P2**:PCBM blend solar cells with different wt ratios..

properties in the blend. The difference in carrier mobility between thin and thick films (**P4** and **P2**) can be clearly attributed to the changes in morphology when films are spin coated or drop cast. The polymer P3 showed no detectable results in CELIV studies, which indicates a rather low mobility $< 10^{-7}$ cm^2/Vs.

One of the important parameters in bulk heterojunction solar cells is the charge carrier mobility. We compared our mobility results with the charge carrier mobilities of the most well-known polymers, MDMO-PPV and P3HT, which were investigated by Mihailetchi et al. and Mozer et al., respectively [24,25,26]. A hole mobility of μ_h=5.10^{-7} cm^2/Vs was reported for MDMO-PPV pristine thin films [24,25] whereas a hole mobility of μ_h=4.10^{-3} cm^2/Vs was reported for P3HT films [25]. Our mobility values lies between these values.

Among the four polymers, **P2**:PCBM solar cells had the highest power conversion efficiency. Therefore, we focused more on solar cells consisting of **P2**:PCBM blends with varying ratio of PCBM (1:1, 1:2, 1:3 and 1:4 wt ratios). Fig. 7 shows the current–voltage characteristics of the solar cells consisting of ITO/PEDOT:PSS/**P2:**PCBM/LiF/Al (with 1:1, 1:2, 1:3 and 1:4 ratios).

The best device performance for **P2** was achieved when **P2** was blended with PCBM in 1:3 wt ratio. The V_{OC} was found to be 800 mV except for the 1:1 wt ratio. Although fill factor of around 0.4 can be regarded as low, the lowest fill factor was found for 1:1 wt ratio. This cell exhibited the lowest power conversion efficiency. The short-circuit current densities were over 3 mA/cm^2. However, the highest short-circuit current density was achieved for **P2** blended in 1:3 wt ratio. To better correlate the photovoltaic performance we also performed morphology and incident photon to current efficiency studies on the **P2**:PCBM solar cells with varying ratios of PCBM. To correlate the morphology of the **P2**:PCBM solar cells to the photovoltaic performance, we performed an AFM study. Fig. 8 shows the images obtained by AFM for **P2**:PCBM films 1:1, 1:2, 1:3, 1:4 wt ratios spin cast from chlorobenzene.

As can be seen from Fig. 8, for the blend films of **P2**:PCBM with 1:1 ratio phase separation can be clearly seen. 100 nm height scale value indicates the coarse granied nanomorphology of the films. The grained nanomorphology in the 1:1 blend film seems to be the main limiting factor which might be an explanation for the low short-circuit currents. For the rest of the blend films of **P2**:PCBM with 1:2, 1:3, and 1:4 ratios, AFM images indicate rather smooth surfaces (5 nm height scale) which is in accordance with the photovoltaic results.

For further understanding, we also performed IPCE studies. Fig. 9 shows the IPCE of **P2**:PCBM blend solar cells with 1:1, 1:2, 1:3 and 1:4 wt ratios.

P2:PCBM blend solar cells with 1:3 wt ratio, as is the case in the photovoltaic results, showed the best performance with an almost 30% IPCE at around 500 nm. The results for 1:2 wt ratio was almost similar to 1:3 wt ratio which is in accordance with the photovoltaic results.

From chemistry point, placing the thiophene ring at the bridge between triple bond and double bond as in **P2** leads to far better photovoltaic performance as when it is placed between two double bonds as in **P1**. Comparable photovoltaic results were obtained for both anthracene-containing polymers **P3** and **P4**, despite the strong differences observed in their charge carrier mobilities. According to the CELIV measurement technique, no charge carrier mobility was detected for **P3**, bearing anthracene between two double bonds, while the highest mobility value among the four materials was obtained for **P4**, where anthracene is at the bridge between triple bond and double bond.

Among these four polymers, **P2** seems to be the most promising. The hydrophobic alkyl side chains act as shield around the conjugated backbone, thereby hinder the movement of charges, as proven by electrochemical studies [27, 28, 29]. Very high side-chain density is disadvantageous in the construct of solar cells due to following reasons: (1) They dilute the concentration of the active conjugated species in the volume unit, so that less photons are absorbed, and (2) they reduce the interfacial area between donor and acceptor components leading to strong phase separation and concomitant poor photovoltaic performance [28]. For instance, by reducing the side-chain density (synonymous to a decrease of the hydrophobicity) in the case of **P2**, we observed a constant increase of the short-circuit current,

Table 2
Thick[(a)] and thin[(b)] film hole mobilities of pristine **P1**, **P2** and **P4** films.

Polymer	μ_{hole} (cm^2/Vs) [(a)]	μ_{hole} (cm^2/Vs) [(b)]
P1	1.6×10^{-6}	1.3×10^{-6}
P2	2×10^{-6}	3×10^{-5}
P4	1.6×10^{-5}	7.1×10^{-5}

J_{SC}, and concomitant increase of the power conversion efficiency, $\eta_{AM1.5}$ of the resulting photovoltaic cells. We attribute this increase to the enlargement of the donor–acceptor interfacial area, large interfacial area between donor and acceptor provides increased charge separation in the case of **P2**. However, the lower filling factor FF of **P2** as well as of **P1**, **P3** and **P4** is an indication that the majority of the dissociated free charge carriers are not effectively transported to the electrodes. The low mobility of holes is a major reason for this poor transport. In addition to this, **P4** exhibits the highest mobility value (Fig. 6 and Table 2), but the lowest energy conversion efficiency of 0.2% among the four studied polymers. Similar effects were also observed by *Kopidakis* et al. [22].

4. Conclusions

We have investigated the hole mobility and photovoltaic performance of two thiophene- as well as two anthracene-containing PPE-PPV polymers. Placing thiophene at the bridge between triple bond and double bond as in **P2** leads to far better solar cell performance than placing thiophene between two double bonds as in **P1**, despite identical absorption of both compounds.

Acknowledgements

Valuable support and discussions by Professor Niyazi Serdar Sariciftci are highly acknowledged. A. Wild and U.S. Schubert are grateful to the Dutch Polymer Institute, and D. A. M. Egbe is grateful to the *Deutsche Forschungsgemeinschaft* (SPP1355) for financial support. Serap Günes acknowledges European Science Foundation (ESF) for an exchange grant. Serap Günes and Emel Cevik acknowledges the financial support of The Scientific and Technological Research Council of Turkey (Tübitak) with the project number 108-T-485.

References

[1] N.S. Sariciftci, Plastic photovoltaic devices, Materials Today 7 (2004) 36–40.
[2] M. Shahinpoor, K.J. Kim, M. Mojarrad, Artificial Muscles, Chapter 8, Conductive or Conjugated Polymers as Artificial Muscles, Taylor and Francis, 2007, pp. 323–324.
[3] S.E. Shaheen, C.J. Brabec, N.S. Sariciftci, F. Padinger, T. Fromherz, J.C. Hummelen, 2.5% efficient organic solar cells, Applied Physics Letters 78 (2001) 841–843.
[4] H. Hoppe, N.S Sariciftci, Organic solar cells: An overview, Journal of Material Chemistry 19 (2004) 1924–1945.
[5] C.J. Brabec, N.S. Sariciftci, J.C. Hummelen, plastic solar cells, Advanced Functional Materials 11 (2001) 15–26.
[6] M Allbrahim, H. Klaus Roth, M. Schroedner, A. Kalvin, U. Zhokhavets, G. Gobsch, P. Scharff, S. Sensfuss, The Influence of the optoelectronic properties of poly(3-alkylthiophenes) on the device parameters in flexible polymer solar cells, Organic Electronics 6 (2005) 65–77.
[7] T. Erb, S. Raleva, U. Zhokhavets, G. Gobsch, B. Stühn, M. Spode, O. Ambacher, Structural and optical properties of both pure poly(3-octylthiophene) (P3OT) and P3OT/fullerene Films, Thin Solid Films 450 (2004) 97–100.
[8] C.N. Hoth, P. Schilinsky, S.A. Choulis, C.J. Brabec, Printing highly efficient organic solar cells, Nanoletters 8 (2008) 2806–2813.
[9] J.A. Hauch, P. Schilinsky, S.A. Choulis, R. Childer, M. Biele, C.J. Brabec, Flexible organic P3HT:PCBM bulk heterojunction modules with more than 1 year outdoor lifetime, Solar Energy Materials and Solar Cells 92 (2008) 727–731.
[10] S.H. Park, A. Roy, S. Beaupré, S. Cho, N. Coates, J.S. Moon, D. Moses, M. Leclerc, K. Lee, A.J. Heeger, Bulk heterojunction Solar, Cells with internal quantum efficiency approaching 100%, Nature Photonics 3 (2009) 297–303.
[11] F.C. Krebs, M. Jorgensen, K. Norrman, O. Hagemann, J. Alstrup, T.D. Nielsen, J. Fyenbo, K. Larsen, J. Kristensen, A complete process for production of flexible large area polymer solar cells entirely using screen Printing-first public demonstration, Solar Energy Materials and Solar Cells 93 (2009) 422–441.
[12] F.C. Krebs, S.A. Gevorgyan, B. Gholamkhass, S. Holdcroft, C. Schlenker, M.E. Thompson, B.C. Thompson, D. Olson, D.S. Ginley, S.E. Shaheen, H.N. Alshareef, J.W. Murphy, W.J. Youngblood, N.C. Heston, J.R. Reynolds, S.J.D. Laird, S.M. Tuladhar, J.G.A. Dane, P. Atienzar, J. Nelson, J.M. Kroon, M.M. Wienk, R.A.J. Janssen, K. Twingstedt, F. Zhang, M. Andersson, O. Inganäs, M.L. Cantu, R. de Bettignies, S. Guillerez, T. Arneuts, D. Cheyns, L. Lutsen, B. Zimmermann, U. Würfel, M. Niggemann, H.F. Schleirmacher, P. Liska, M. Grätzel, P. Lianos, E.A. Katz, W. Lohwasser, B. Jannon, A Round Robin, Study of flexible large-area roll-to roll processed polymer solar cell modules, Solar Energy Materials and Solar Cells 93 (2009) 1968–1977.
[13] F.C. Krebs, S.A. Gevorgyan, J. Alstrup, A Roll-to-Roll, Process to flexible polymer solar cells: model studies, manufacture and operational stability studies, Journal of Materials Chemistry 19 (2009) 5442–5451.
[14] M. Jorgensen, K. Norrman, F.C. Krebs, Stability/degradation of polymer solar cells, Solar Energy Materials and Solar Cells 92 (2008) 686–714.
[15] F.C. Krebs, Fabrication and processing of polymer solar cells: a review of printing and coating techniques, Solar Energy Materials and Solar Cells 93 (2009) 394–412.
[16] M. Scharber, D. Mühlbacher, M. Koppe, P. Denk, C. Waldauf, A.J. Heeger, C. Brabec, Design rules for donors in bulk heterojunction solar cells- towards 10% energy-conversion efficiency, Advanced Materials 18 (2006) 789–794.
[17] A. Wild, D.A.M. Egbe, E. Birckner, V. Cimrová, R. Baumann, U.-W. Grummt, U.S. Schubert, Anthracene and thiophene containing MEH–PPE–PPVS: synthesis and study of the effect of the aromatic ring position on the photophysical and electrochemical properties, Journal of Polymer Science Part. A: Polymer Chemistry 47 (2009) 2243–2261.
[18] R.O Garay, H. Naarmann, K. Müllen, Synthesis and characterization of poly(1,4-anthrylenevinylene), Macromolecules 27 (1994) 1922–1927.
[19] Thesis David Mühlbacher, Johannes Kepler University Linz (2002).
[20] X. Yang, J. Loos, S.C. Veenstra, W.J.H. Verhees, M. Wienk, M. Kroon, M.H.J. Michels, R.A.J. Janssen, Nanoscale morphology of high performance polymer solar cells, Nanoletters 5 (2005) 579–583.
[21] H. Hoppe, N.S. Sariciftci, Polymer solar cells, Advanced Polymeric Science 214 (2008) 1–86.
[22] N. Kopidakis, W.J. Mitchell, J. Lagemaat, D.S. Ginley, G. Rumbles, S.E. Shaheen, W.L. Rance, Bulk heterojunction organic photovoltaic devices based on phenyl cored thiophene dendrimers, Applied Physics Letters 89 (2006) 103524–103527.
[23] R. Pacios, J. Nelson, D.D.C. Bradley, C.J. Brabec, Composition dependence of electron and hole transport in polyfluorene:[6,6]-phenyl c_{61}-butyric acid methyl ester blend films, Applied Physics Letters 83 (2003) 4764–4767.
[24] V. Mihailetchi, J.K.J. van Duren, P.W.M. Blom, J.C. Hummelen, J R.A. Janssen, J.M. Kroon, M.T. Rispens, W.J.H. Verhees, M.M. Wienk, Electron transport in a methanofullerene, Advanced Functional Materials 13 (2003) 43–46.
[25] A.J. Mozer, N.S. Sariciftci, A. Pivrikas, R. Österbacka, G. Juška, L. Brassat, H. Bässler, Charge carrier mobility in regioregular poly(3-hexylthiophene) probed by transient conductivity techniques: A comparative study, Physical Review B 71 (2005) 035214–035223.
[26] A.J. Mozer, P. Denk, M.C. Scharber, H. Neugebauer, N.Serdar Sariciftci, Novel Regiospecific MDMO-PPVCopolymer with Improved Charge Transport for Bulk, Heterojunction Solar Cells, Journal of Physical Chemistry B 108 (2004) 5235–5242.
[27] D.A.M. Egbe, L.H. Nguyen, H. Hoppe, D. Mühlbacher, N.S. Sariciftci, Side chain influence on electrochemical and photovoltaic properties of yne-containing poly(phenylenevinylene)s, Macromolecular Rapid Communication 26 (2005) 1389–1394.
[28] Z.-K. Chen, W. Huang, L.H. Wang, E.T. Kang, B.T. Chen, C.S. Lee, S.T. Lee, A family of electroluminescent silyl-substituted poly(p-phenylenevinylene)s: synthesis, characterization, and structure-property relationships, Macromolecules 33 (2000) 9015–9025.
[29] T. Yamamoto, B.L. Lee, New soluble coplanar poly(naphthalene-2-6, diyl) type π-conjugated polymer, poly(pyrimido [5,4-d] pyrimidine-2,6-diyl), with nitrogen atoms at all of the o-positions, Synthesis, solid structure, optical properties, self assembling phenomena, and redox behavior, macromolecules 35 (2002) 2993–2999.